Instant WS2 platelets reorientation of self-adaptive WS2/a-C tribocoating

Cao, Huatang; Wen, Feng; De Hosson, J.T.M.; Pei, Yutao T.

Published in:
Materials Letters

DOI:
10.1016/j.matlet.2018.06.111

Publication date:
2018

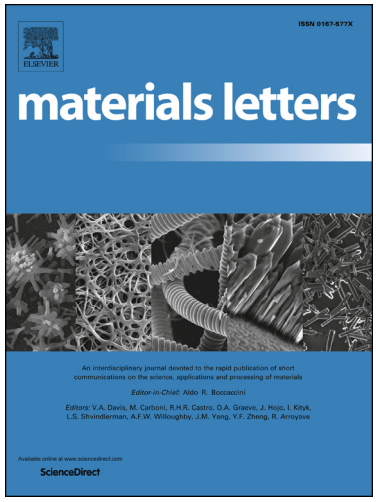

Instant WS_2 platelets reorientation of self-adaptive WS_2/a-C tribocoating

Huatang Cao, Feng Wen, J.Th.M. De Hosson, Y.T. Pei

PII: S0167-577X(18)31016-4
DOI: https://doi.org/10.1016/j.matlet.2018.06.111
Reference: MLBLUE 24551

To appear in: *Materials Letters*

Received Date: 16 March 2018
Revised Date: 28 May 2018
Accepted Date: 24 June 2018

Please cite this article as: H. Cao, F. Wen, h.M.D. Hosson, Y.T. Pei, Instant WS_2 platelets reorientation of self-adaptive WS_2/a-C tribocoating, *Materials Letters* (2018), doi: https://doi.org/10.1016/j.matlet.2018.06.111

Instant WS_2 platelets reorientation of self-adaptive WS_2/a-C tribocoating

Huatang Cao [a], Feng Wen [a, b], J.Th.M. De Hosson [c], Y.T. Pei [a*]

[a] Department of Advanced Production Engineering, Engineering and Technology Institute Groningen, University of Groningen, Nijenborgh 4, 9747AG, The Netherlands.

[b] School of Materials and Chemical Engineering, Hainan University, Haikou, 570228, China.

[c] Department of Applied Physics, Zernike Institute for Advanced Materials, University of Groningen, Nijenborgh 4, 9747AG Groningen, The Netherlands.

Abstract:

WS_2/a-C nanocomposite coatings were deposited by magnetron co-sputtering using WS_2 and graphite targets. The microstructure and triboperformance of the coatings were scrutinized via microscopy (AFM, SEM, FIB, HRTEM), spectroscopy (XRD, XPS) and tribometry. Atomic WS_2 platelets are randomly embedded in an amorphous carbon matrix of the as-deposited nanocomposite coating. HRTEM observations of tribofilm/transfer layer reveal that the sliding contact immediately reorients WS_2 platelets parallel to the sliding interface and thereby leads to self-adaptive "frictionless" response. The coefficient of friction falls to 0.02 in dry air and reaches 0.10 in humid air, and is reversible as testing atmosphere cycles between dry air and humid air.

Keywords: WS_2; Nanocomposites; Magnetron sputtering; Self-adaptation; Reorientation; Self lubrication

1. Introduction

Transition metal dichalcogenides (TMD) are well known for their solid lubricating behavior and are applied widely in aerospace industry [1–3]. Their MX_2-type structure is highly anisotropic. For instance, WS_2 crystallizes in the hexagonal units where layers of W atoms are sandwiched in-between layers of packed sulphur atoms. The bonding within each unit, i.e. the M-X bond is covalent, while the different units are held together by weak Van der Waals interactions [4]. The ultralow shear strength (1-2 MPa) in (002) orientation renders an easy glide of each WS_2 layer, yielding an ultralow friction [1,5].

However, pure WS_2 coatings prepared by sputtering exhibit porous structure and degrade their lubricating properties through oxidizing in moisture [6]. This is because the edge-plane orientation of WS_2 readily suffers from oxidations due to the passivation of their dangling bonds and active sites. Fortunately, edge-oriented or even amorphous WS_2 can adapt itself during a sliding contact forcing nano-laminae to favor the frictionless orientation where their basal planes are parallel to the sliding

* Corresponding author. E-mail address: y.pei@rug.nl

direction [1,4]. Their wear resistance is also limited due to the low hardness and poor load-bearing capacity. Therefore nanostructured tribocoatings consisting of WS_2 nano-lubricant embedded in an amorphous carbon (a-C) matrix are designed to impart ultralow friction, high wear resistance and self-adaptive response to various tribological conditions.

2. Experimental procedures

WS_2/a-C nanocomposite coating was deposited on single crystal silicon(100) wafers, with non-reactive magnetron sputtering in a TEER UDP400/4 closed-field unbalanced magnetron sputtering system that consisted of four magnetron/targets vertically arranged on the four sides of the chamber. The substrates were mounted vertically on a carousel holder that rotated at 3 rpm in front of the targets (80 mm apart). The substrates were first ultrasonically cleansed in acetone and Ar plasma etched for 20 min at −400 V bias voltage (pulsed DC mode). Two WS_2 targets powered at 0.5A (150 kHz pulsed DC power, 62.5 % duty cycle) and one graphite target (0.5A DC) were co-sputtered at a pressure of 0.6 Pa for the deposition of WS_2/a-C nanocomposite coating. A 300 nm thick Cr interlayer was first deposited to enhance the interfacial adhesion between the top coating and Si substrate. The deposition time was 2h to produces 2 µm thick coating. No additional substrate heating was applied during deposition.

The microstructure of the coating and the tribofilm were scrutinized using an atomic force microscope (AFM, Dimension 3100), high-resolution/energy-filtering transmission electron microscope (HR-TEM/EF-TEM, JEOL JEM-2010F operated at 200 kV) and EDS-enabled scanning electron microscope (ESEM, Philips XL30-FEG). The phases were examined by grazing incidence X-ray diffraction (GIXRD, PANalytical-X'Pert MRD) at 2° incident angle. The chemical bonding was estimated by an X-ray photoelectron spectroscopy (XPS, Surface Science SSX-100 ESCA) using Al Kα (± 0.1 eV). To identify the original surface chemistry, no prior Ar+ sputter cleaning of the surface was executed. The tribo-performance was evaluated using a CSM ball-on-disk tribometer against ø6 mm 100Cr6 ball at a sliding speed of 10 cm/s. A 5N normal load generates a Hertz contact pressure of 0.75 GPa. The tribotests were run for 10000 laps in dry air (5% relative humidity, H_R, wear track diameter 15 mm) and humid air (55% H_R, wear track diameter 18 mm), respectively. In another tribotest with a wear track diameter 15 mm the humidity was alternated (5% ↔ 55% H_R) four times. Confocal images of the wear tracks were captured to evaluate the wear rate (W_r). Focused ion beam (FIB, Lyra Tescan) was employed to prepare TEM lamella on the wear tracks.

3. Results and discussions

3.1. Microstructure characterization.

AFM image displayed in Fig. 1a shows that the WS_2/a-C coating has a dome-like morphology typical for sputtered DLC coatings (RMS roughness: 8.1 nm). As an indication, EDS analysis estimated the atomic composition of the coating as 16C-52S-30W-2O, pointing to a slightly

substoichiometric S/W ratio of 1.73. HRTEM in Fig. 1b reveals that short WS_2 platelets are randomly distributed in an amorphous carbon matrix, with the inset showing the selected area diffraction pattern (SADP) of random WS_2 platelets, which consists of a broad circular band reflecting the 10Z (z = 1, 2, 3…) planes besides the (002) and (110) diffraction rings. The GIXRD pattern in Fig. 1c indicates (002) WS_2 basal plane located at 2θ = ~14°, compatible with the JCPDS card (No. 008-0237). Besides, an asymmetrical (100) peak at 2θ = 33° with a long tail towards high angles suggesting reflections of the 10Z planes [7], confirming the diffraction halo in the SADP (Fig. 1b). Besides, comparison with the sharp diffraction peaks of pure WS_2 coating confirms the nanocomposite nature of WS_2/a-C.

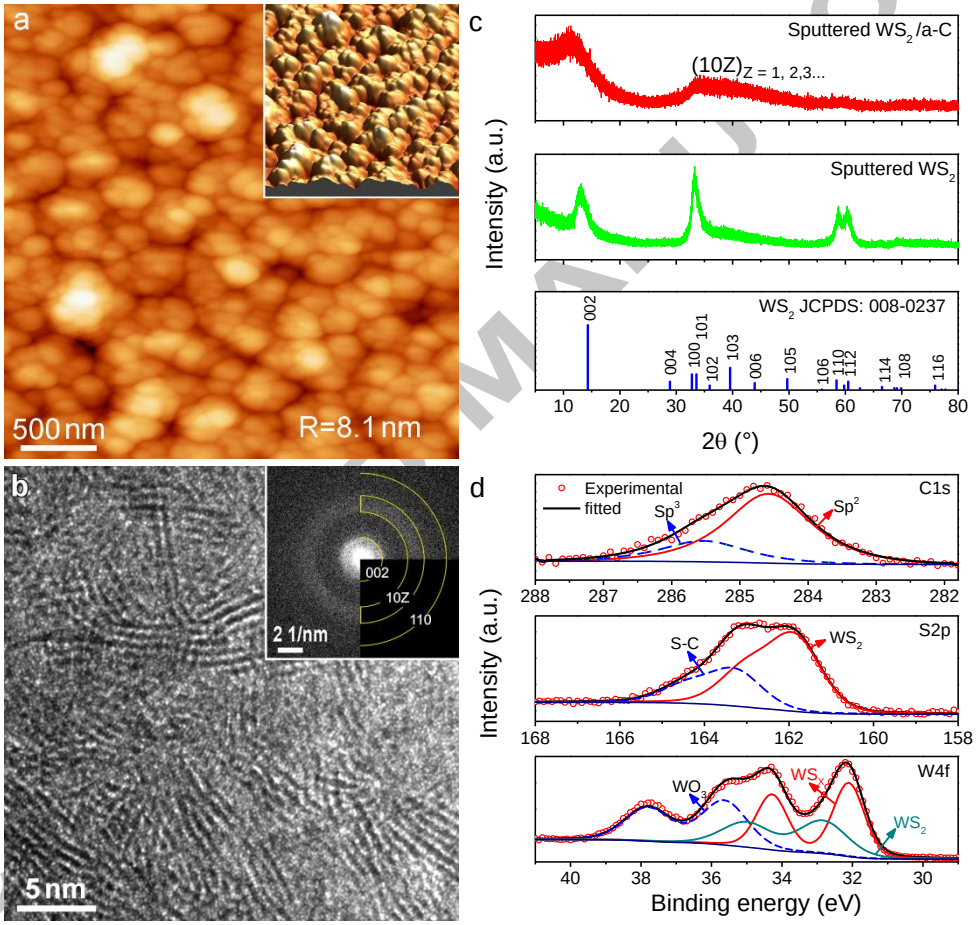

Fig. 1. (a) AFM scan showing the surface morphology of WS_2/a-C coating; (b) HR-TEM micrograph of short WS_2 platelets and SADP in the inset; (c) GIXRD spectra of WS_2/a-C and pure WS_2 coatings; (d) XPS deconvolutions of C1s, S2p and W4f peaks.

Fig. 1d shows the XPS spectra of deconvoluted C1s, S2p, W4f peaks. Two singlets at 284.6 eV and 285.5 eV correspond to sp^2 and sp^3 of the amorphous carbon matrix [4]. The sp^3/sp^2 ratio is 0.3 and indicates that sp^2 (C=C) bond is prevalent, corresponding to a hardness of around 5.0 GPa [6]. Deconvolution of the S2p doublet at 161.9 eV corresponds to S-W bonds [4]. Another pair at 163.6 eV is assigned to S-C bond existing at the interface between the WS_2 and the matrix [4,8]. The $W4f_{7/2}$ peak at 32.8 eV and 32.1 eV correspond to WS_2 and WS_x (x < 2) [4,8] and validates the S deficiency.

The W-O bond at 35.6 eV is attributed to WO_3 which comes from both coating contaminations and surface oxidizing [4,9].

3.2. Tribological properties

Fig. 2a shows the coating tribo-performance sliding in dry (relative humidity H_R = 5%) and humid air (H_R = 55%), respectively. The coefficient of friction (CoF) rapidly falls to an ultralow value of 0.02 in dry air and it remains nearly constant. However, when the humidity rises to 55% H_R, the CoF increases and fluctuates at 0.10, correlated with a wear rate of 5.3×10^{-7} mm^3 $N^{-1}m^{-1}$ as compared to 2.9×10^{-7} mm^3 $N^{-1}m^{-1}$ in dry air. More strikingly, Fig. 2b shows a self-adaptive behavior against humidity alternation as CoF can be reversible from 0.02 to 0.11 when the dry air and humid air are switched multiple times (each period lasts 2000 laps). Upon each environmental cycle from dry air to humid air, the CoF promptly jumps to the range of 0.13 - 0.14, followed by a gradual decrease down to ~0.09. The CoF immediately recovers to 0.02 again once the atmosphere reverses from the humid air to dry air. The rapid switch and maintained CoFs (Fig. 2b) in the long cyclic sliding suggest such self-adaptation to work environment independent of the accumulating effects from previous sliding.

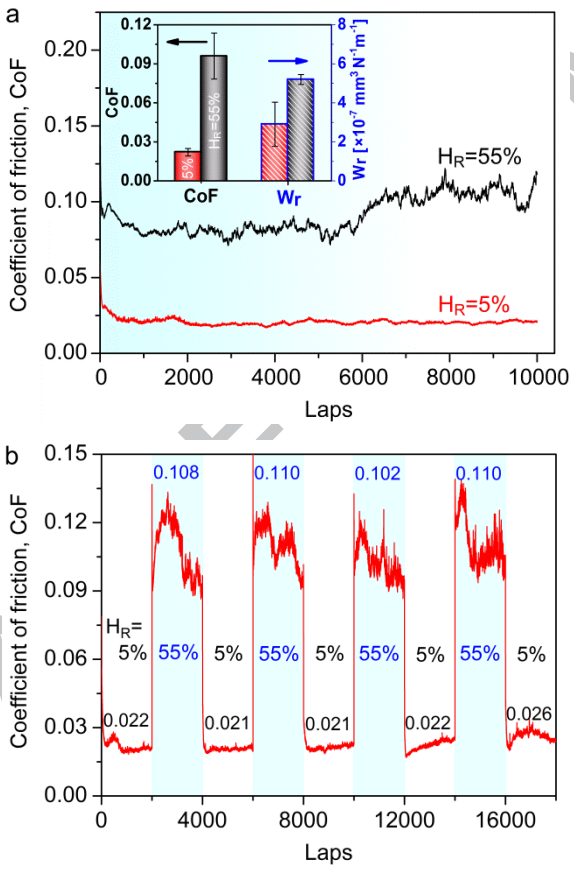

Fig. 2. Triboperformance of WS_2/a-C coating: (a) CoF under 5% H_R and 55% H_R, respectively, with the inset showing the average CoF and W_r; (b) self-adaptation to humidity variations between 5% and 55% H_R.

3.3. Self-adaptive mechanism

Fig. 3a and b show that a tribofilm, up to 150 nm thick, formed substantially on the wear track. Combined EF-TEM mappings presented in Fig. 3c manifest the enrichment of O, W at the coating/tribofilm interface. The intensity of O is more prominent in the tribofilm as compared to that in the as-deposited coating, which indicates partial oxidation in the sliding process. Fig. 3d and e confirm that characteristic WS_2 basal planes formed are well aligned parallel to the sliding direction, that is, to the interface between the tribofilm and the coating. The measured d-spacing of the WS_2 basal planes is 0.65 nm, slightly larger than the JCDPS value of 0.63 nm due to the carbon doping into the hexagonal lamella. Notably, in Fig. 3d one can distinguish the long range ordered WS_2 platelets (> tens of nm) along the interface from the short range randomized ones underneath the unaffected coating. In addition, a 5-nm thick layer containing nanocrystalline WO_3 forms surprisingly between the original coating and the tribofilm, in agreement with EF-TEM results. This rarely reported sandwiched WO_3 layer implies that WS_2 oxidizes to form WO_3 in the turbulent running-in period. WO_3 soon disappears once basal WS_2 planes are fully realigned and start to play a critical role as antioxidant. However, small amounts of WO_3 nanocrystallites (circled in Fig. 3f and confirmed by the inset SADP) occur in the middle of tribofilm where the WS_2 platelets become less aligned. The tribofilm also appears moderately aligned at the outmost surface, as shown in Fig. 3g. Similarly, Fig. 4a confirms thick (002)-orientated WS_2 layers are transferred onto the counterpart ball.

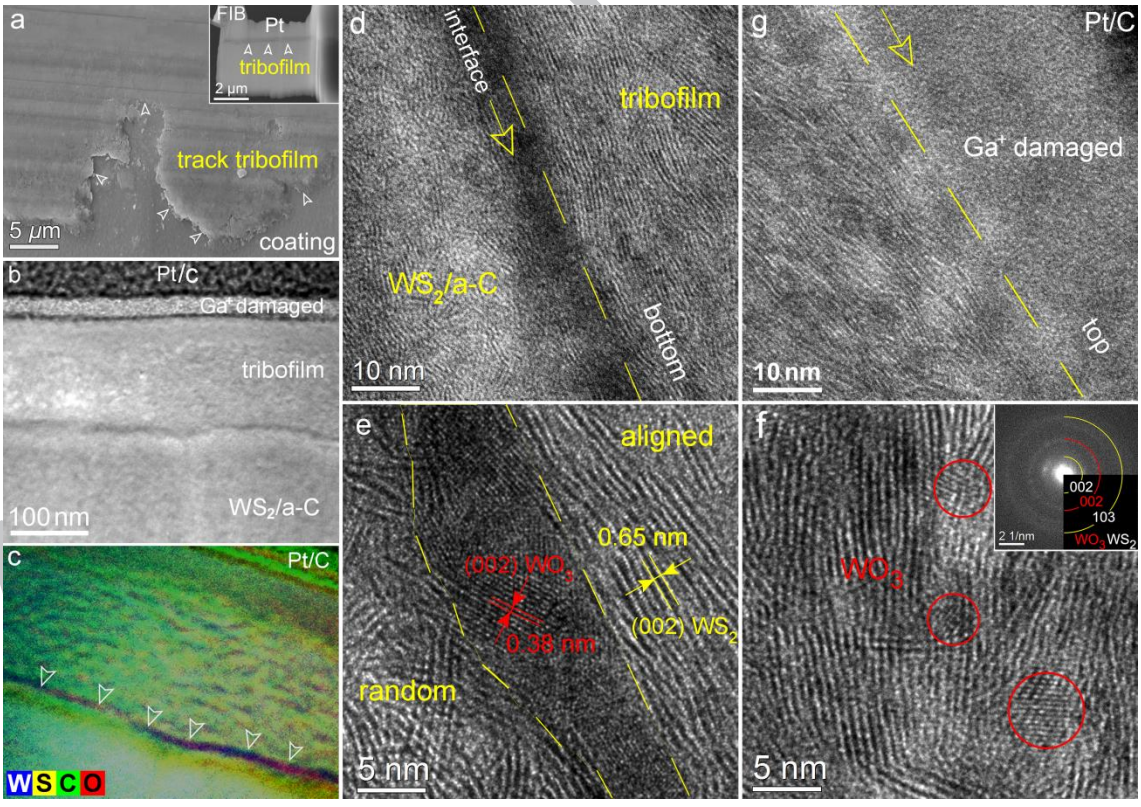

Fig. 3. (a) SEM top view of the tribofilm formed on the wear track at 5% H_R with the inset showing the FIB-cut X-TEM lamellae; (b, c) X-TEM micrograph of the tribofilm and related EFTEM elemental mapping; (d, e) HRTEM images elucidating the reorientation of WS_2 basal planes in the tribofilm; (f) HRTEM image of WO_3 in the middle of the tribofilm and the corresponding SADP in the inset; (g) HRTEM image of the topmost tribofilm.

Previous study [4,10,11] reported that amorphous TMDs crystallize initially from the bottom of the wear track and become mostly ordered at the outmost tribofilm. On the contrary, Fig. 3d-e and Fig. 4b reveal that an immediate perfect reorientation of WS_2 occurs directly at the wear interface including both the wear track and the wear scar. The extremely short running-in period evidenced by a rapid drop of CoF to 0.02, as shown in Fig. 2, indicates the synchronization of WS_2 platelets alignment with the frictional contact. The coating thus reacts in an immediate self-adaptation to loading condition and environmental change by forming lubricative tribolayer.

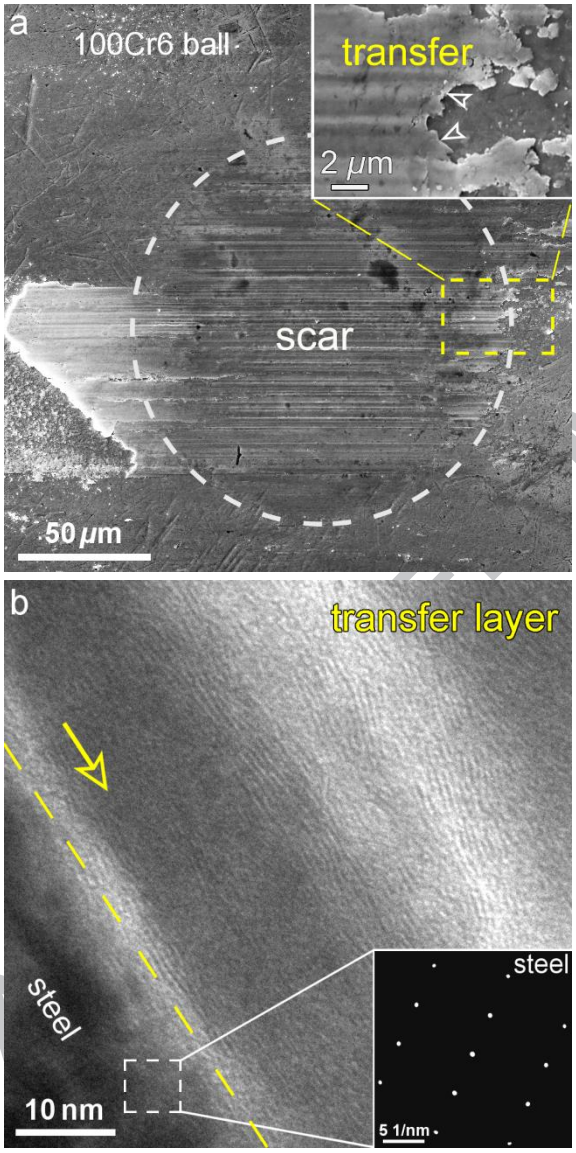

Fig.4. (a) SEM micrograph showing the transfer layer on the wear scar of 100Cr6 counterpart ball; (b) Cross-section HRTEM image revealing well-realigned WS_2 platelets in the transfer layer.

It is known that a lubricating tribolayer blocks direct metal/coating contact and offers self-lubrication. In particular, the shearless (002)-oriented WS_2 tribolayers impart exclusive lubrication [1]. Nevertheless, Fig. 3f indicates that formed WO_3 nanocrystallites break up and even terminate the

continuous reordering process. They interrupt the steady super-lubricity, as confirmed by the fluctuating CoF tested in 55 % H_R (see Fig. 2a). FIB-cut on wear tracks in humid air even shows no clear reorientation of WS_2 platelets in this case (not shown). Water attacks leading to high shear strength during humid sliding may further worsen the lubrication [12]. However, the graphitization of a-C matrix during sliding in humid air [3,6,10] may simultaneously compensates the weakened lubrication of WS_2 and help retain a still low CoF in ambient air.

4. Conclusions

WS_2/a-C nanocomposite coatings, with short WS_2 platelets randomized in an amorphous carbon matrix, were prepared by magnetron co-sputtering. CoF reaches 0.02 and 0.10 in dry and humid air respectively. During frictional contact WS_2 basal planes despite sulfur substoichiometry can be instantly aligned parallel to the sliding direction. Such reoriented WS_2 platelets in the tribofilm/transfer-layer provide superior lubrication and enhanced inertness to oxidation. WS_2/a-C coatings become tribologically self-adaptive to humidity variations.

5. Acknowledgments

H.T. Cao acknowledged China Scholarship Council for financial support (CSC, No. 201406160102).

References

[1] C. Muratore, A.A. Voevodin, Annu. Rev. Mater. Res. 39 (2009) 297–324.

[2] S. V. Prasad, T.J. Renk, P.G. Kotula, T. DebRoy, Mater. Lett. 65 (2011) 4–6.

[3] A.A. Voevodin, J.P. O'Neill, J.S. Zabinski, Surf. Coat.Technol. 116–119 (1999) 36–45.

[4] J. Sundberg, H. Nyberg, E. Särhammar, F. Gustavsson, T. Kubart, T. Nyberg, et al., Surf. Coat.Technol. 232 (2013) 340–348.

[5] J.S. Wu, X.L. Liu, L.M. Yan, L. Zhang, Mater. Lett. 196 (2017) 414–418.

[6] H. T. Cao, J.Th.M De Hosson, Y.T. Pei, Surf. Coat.Technol. 332 (2017) 142–152.

[7] G. Weise, N. Mattern, H. Hermann, A. Teresiak, I. Bächera, W. Brücknera, et al, Thin Solid Films. 298 (1997) 98–106.

[8] J.F. Moulder, J. Chastain, Handbook of X-ray Photoelectron Spectroscopy: A Reference Book of Standard Spectra for Identification and Interpretation of XPS Data, Physical Electronics Division, Perkin-Elmer Corporation, 1992.

[9] A. Katrib, F. Hemming, P. Wehrer, L. Hilaire, G. Maire, J. Electron. Spectrosc. Relat. Phenom. 76 (1995) 195–200.

[10] S. Cai, P. Guo, J.Z. Liu, D. Zhang, P.L. Ke, A.Y. Wang, et al.,Tribol. Lett. 65 (2017). 79-90.

[11] J. Xu, T.F. He, L.Q. Chai, L. Qiao, X.Q. Zhang, P. Wang, et al., Phys. Chem. Chem. Phys. 19 (2017) 8161–8173.

[12] E. Serpini, A. Rota, A. Ballestrazzi, D. Marchetto, E. Gualtieri, S. Valeri, Surf. Coat. Technol. 319 (2017) 345–352.

Highlights:

1. WS_2/a-C nanocomposite coatings were deposited by magnetron co-sputtering graphite and WS_2 targets
2. The coefficient of friction falls to 0.02 in dry air and reaches 0.10 in humid air
3. Instantly reorienting WS_2 platelets parallel to the sliding direction leads to ultralow friction in dry air.
4. Coatings tend tribologically self-adaptive to humidity variations